Quantum confinement effect on Gd_2O_3 clusters

B. Mercier, G. Ledoux,[a] and C. Dujardin
LPCML CNRS UMR 5620, Université de Lyon, Université Claude Bernard Lyon I, 10 rue A. M. Ampère, 69622 Villeurbanne Cedex, France

D. Nicolas, B. Masenelli, and P. Mélinon
LPMCN CNRS UMR 5586, Université de Lyon, Université Claude Bernard Lyon I, 6 rue A. M. Ampère, 69622 Villeurbanne Cedex, France

G. Bergeret
IRC CNRS UPR 5401, 2 rue A. Einstein, 69626 Villeurbanne Cedex, France

(Received 23 May 2006; accepted 11 December 2006; published online 26 January 2007)

The evolution of the gap of a nanoscaled insulator material, namely, Gd_2O_3, has been observed by means of vacuum ultraviolet excitation spectra of a dopant (Eu^{3+}). The nanoparticles have been synthesized by the low energy cluster beam deposition technique and grown afterward by different annealing steps. A gap shift towards the blue is observed, similar to what is observed in semiconductor nanoparticles. Despite the strong ionic character of the material, the evolution exhibits a behavior similar to covalent materials. The evolution of the gap for Gd_2O_3 follows the same empiric rule that has been derived for semiconductors (ZnO, CuBr, Si, and CdS). It shows that, in spite of the strong ionic character of the material (0.9 on the scale of Phillips), the amount of covalency is important enough for creating a significant delocalization of the electron with regard to its hole. © *2007 American Institute of Physics*. [DOI: 10.1063/1.2431366]

I. INTRODUCTION

In the last 15 years many works have been devoted to the study of the optical properties of materials at the nanometer range.[1,2] In particular, quantum confinement effects have been of particular interest since they offer the possibility to tune the optical properties over a large wavelength range in the case of semiconductors. Thus nanocrystals of CdS and CdSe are now commonly used for biological labeling.[3] Compared to biological molecules they offer the advantage of needing only one wavelength to excite all particles. However, they also have some drawbacks. For instance, the emission band is still quite large (typically a few tens of nanometers). Moreover, their emission is not stable under a high excitation power and a careful passivation of their surface is necessary in order not to quench the luminescence.

On a fundamental point of view, the description of quantum confinement in such materials is based on the effective mass approximation (EMA).[4] This model is adapted to pure covalent or slightly ionic materials, where the electron and hole are delocalized over several nanometers. Nevertheless the analytic simple model is unable to reproduce accurately the dependance of the gap as a function of the particle size. One often has to turn to more complex *ab initio* calculations.[5]

A completely different system is given by van der Waals materials such as rare gas solids. For this kind of systems we also came to quite good an understanding thanks to extensive work on rare gas clusters (see, for instance, Ref. 6 and references therein).

In between these two extreme cases, the study of confinement effects in highly ionic materials are much less studied. The question arises whether similar effects of gap modification can appear in these materials and if so to what extent.

Already some results have been obtained for ZnO by Makino *et al.*[7] But insulators with even stronger ionicities are still uninvestigated. In a previous paper,[8] we presented the first observation of the gap blueshift of $Gd_2O_3:Eu^{3+}$ nanoparticles obtained by a sol-lyophilization process. This material is pretty interesting since it has a very high ionicity (0.9), much higher than the Van Vechten-Phillips[9] critical ionicity (0.79) which defines the limit between ion-covalent and ionic materials. The results obtained showed a very small shift of the gap since we could only access to rather big particles. Besides, because the samples were made of agglomerated powders, the determination of the gap was rather difficult. In order to compare the evolution between such a material and the semiconductors we needed to have a variation over a larger range of sizes and, in particular, extend the range towards the smaller sizes. Therefore $Gd_2O_3:Eu^{3+}$ nanocrystals have been grown using a cluster deposition technique which produces smaller particles.

Investigating and understanding these materials are not only of academic interest but also of technological importance for advanced phosphor and photonic applications and many studies have already been devoted to study the luminescence of this kind of materials[10–15] but never focused on the quantum confinement effects.

[a]Author to whom correspondence should be addressed. Tel.: +33 4 72 44 83 38; Fax: +33 4 72 43 11 30; Electronic mail: ledoux@pcml.univ-lyon1.fr

The manuscript is divided in four sections; the first one presents the method of synthesis as well as the different structural characterizations that we performed. The second part is devoted to the study of the growth of the particles through different annealing steps and the corresponding structural characterization. The third part deals with the spectroscopic characterization in the vacuum ultraviolet (VUV) wavelength range. Finally the results are discussed together with the results from the literature for other materials in the last section.

II. SYNTHESIS AND STRUCTURAL CHARACTERIZATION

The nanocrystals have been grown by the low-energy cluster beam deposition technique which has been described in details in previous papers.[16,17] Briefly a target made of pressed powder from the desired composition (Gd_2O_3 $+Eu_2O_3$) is hit by a focalized and pulsed laser (Nd-doped yttrium aluminum garnet second harmonic at 532 nm, pulse duration 5 ns, 10 Hz repetition rate). The pulse creates a plasma of the species which are present in the target. A synchronized helium burst quenches the plasma, triggers the growth of the particles, and flows them downstream through a nozzle. The particles are afterward skimmed to a low pressure vacuum chamber to form a molecular beam of noninteracting clusters. The clusters are deposited smoothly on different substrates for further analysis: LiF for optical analysis, carbon grids for transmission electron microscopy (TEM), and Si wafers for x-ray photoelectron spectroscopy (XPS) measurements.

The TEM analysis has been performed with a Topcon microscope particularly adapted for high resolution measurements. The typical diameter derived from TEM images is 3 nm with 80% of the clusters between 2.6 and 3.5 nm (see Ref. 16). The clusters are crystallized in the cubic ($Ia3$ group 206) phase which is the stable structure of Gd_2O_3 at room temperature and pressure. Despite the very small size of the clusters, the crystal structure does not change to the high temperature stable monoclinic structure ($C2/m$). A detailed explanation of the structure stability is done in Ref. 16. The electronic states of the constituents have been investigated with a CLAM 4 VG x-ray photoelectron spectrometer with a mean resolution of 0.2 eV using the Al K line at 1486.6 eV. The spectra have been corrected from the background according to Shirley's procedure. The XPS sample has been deposited under ultrahigh vacuum conditions on a Si wafer previously cleaned from its silica layer by HF cleaning and Ar^+ sputtering. From the $Eu(3d_{5/2})/Gd(3d_{5/2})$ ratio we determined a doping concentration of 15% which is close to the 10% of the target disk. The spectra of the O1s electron presents two peaks at 530.3 and 532.3 eV with a relative intensity of 0.8 (see Fig. 1). The first peak corresponds to Gd_2O_3 and the second is due to the contamination of the cluster surface by OH as reported by Ref. 18 on bulk Gd_2O_3. The high amount of $Gd(OH)_3$ is due to the large surface to volume ratio of the clusters (40%). The ratio between $Gd(3d_{5/2})$ and O(1s) is coherent with this explanation. From high resolution TEM (HRTEM) and XPS analysis we conclude that this generator produces clusters crystallized in the cubic phase with their surface contaminated by $Gd(OH)_3$. This surface contamination is even larger when the clusters are exposed to air. However, gently annealing the clusters at 300 °C induces a decontamination of the sample as demonstrated in Ref. 16.

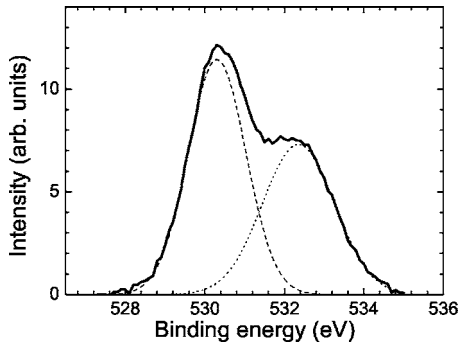

FIG. 1. Binding energy of the 1s electron of oxygen in Eu^{3+} doped Gd_2O_3 clusters deposited under UHV conditions.

III. GROWTH OF THE CLUSTERS

In order to study the variation of the optical properties versus the size we needed to control the size of the clusters over a large range. Therefore we applied different thermal treatments from 400 to 600 °C and looked at the evolution of the different kinds of samples with temperature.

After thermal treatment under vacuum of the TEM grids the particles are kept crystalline and get bigger showing some agglomeration and some sintering as evidenced by Fig. 2. However, on TEM grids the particles are not originally agglomerated and need to diffuse on the grid before sintering can occur. Therefore we are not sure that the obtained sizes are the same as the ones on 150 nm thick samples deposited on cleaved LiF substrates. That is why we analyzed the sample used for optical studies by x-ray diffraction (XRD). We used a powder diffractometer Panalytical X'Pert Pro MPD in a Bragg Brentano configuration. Since we are dealing with very thin films it was difficult to get a nice signal from the XRD in a reasonable time but since we know by TEM that the particles are crystalline it is reasonable to think that the peaks that we observe are due to diffraction lines from the nanocrystals. We could measure the width of two diffraction lines (222 and 400) for the four higher annealing temperatures as can be seen in Fig. 3. For lower temperatures we did not manage to get any signal. By analyzing the width

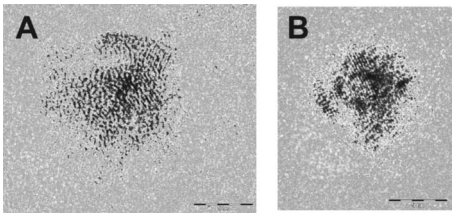

FIG. 2. HRTEM observation of two particles for a 450 °C vacuum-annealed deposit on a TEM grid. (A) Agglomeration of different clusters with atomic planes in different directions and partial sintering. (B) A 10 nm sintered cluster.

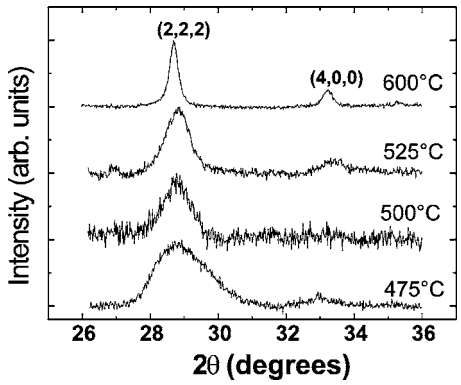

FIG. 3. X-ray diffraction spectra of different annealed samples of Gd_2O_3:Eu clusters.

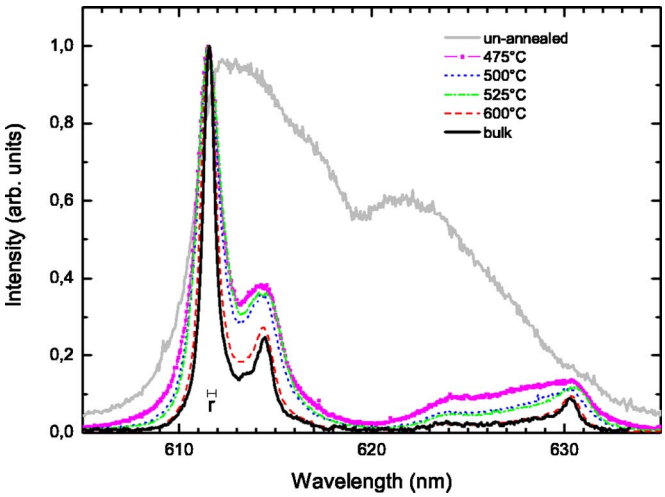

FIG. 4. Emission of different cluster deposits for different annealing temperatures measured at 15 K under 190 nm excitation compared with the emission of a bulk $Gd_2O_3:Eu^{3+}$ sample excited under the same conditions. The small tick labeled *r* denotes the resolution of the experiment.

of the two lines by the Scherrer equation, the average sizes of the crystallites could be derived. For both lines similar sizes are found which shows that there is only a small contribution of strain to the width of the x-ray diffraction peaks. Because of the low signal to noise ratio it was impossible to apply a more sophisticated analysis technique of the data (such as a Rietveld refinement). The results are reported on Table I. Those thermal treatments are well below the melting temperature of the two pure sesquioxides Gd_2O_3 and Eu_2O_3 so segregation of the elements is unlikely. Besides the spectroscopy of the resulting samples is typical of nice cubic europium doped gadolinium oxide; in particular, no emission from surface states is observed.

The size evolution is also evidenced in the spectroscopy of Eu^{3+} as will be discussed afterward.

IV. GAP EVOLUTION WITH THE SIZE: VACUUM ULTRAVIOLET SPECTROSCOPY

Gap values are most often obtained through absorption experiments which is the most direct technique for this kind of study. When the samples got thinner, the technique can be optimized by taking advantage of the Brewster's angle absorption. However, for very thin samples with a high porosity, such as ours, even this optimization becomes awkward. This is the reason why we have turned to a less direct but more efficient technique, namely, the excitation spectroscopy. The details of the latter technique are discussed below.

To get the gap value of the bulk a powder of undoped Gd_2O_3 has been measured using the well known emission from the $^6P_{7/2} \rightarrow {}^8S_{7/2}$ transition of Gd^{3+} peaking at 311 nm. For the measure of the nanoparticle gap, the emission from Gd^{3+} is not intense enough. We therefore needed to use another luminescent probe. The best candidate is Eu^{3+} since it has a very close ionic radius to Gd^{3+}, and can easily be incorporated into the gadolinium oxide matrix with very low modifications of the structure of the matrix. Then we used the very intense $^5D_0 \rightarrow {}^7F_2$ emission transition of Eu^{3+} around 611 nm to monitor the changes in absorption of the matrix.

TABLE I. Different diameters estimation in nanometers as a function of the temperature of annealing by TEM for the unannealed sample and by XRD for the other samples.

Temperature (°C)	Crystallite size (nm)
RT	3
475	5.3
500	9.1
525	10.6±0.3
600	28.7±2.3

VUV experiments were carried around $T=10$ K at the synchrotron radiation beamline Superlumi of the DESY facility at Hamburg, Germany. Emission spectra were performed at an excitation wavelength of 190 nm and by detecting the photoluminescence through an Acton Research Corporation (ARC) monochromator with a 1200 grating/mm grating and a nitrogen cooled charge coupled device detector ensuring a resolution of 0.4 nm. For excitation spectra of the $Gd_2O_3:Eu^{3+}$ deposited clusters, the emission range was selected using an ARC monochromator with a 300 grating/mm grating and 3.5 mm for both entrance and exit slits which ensures a spectral resolution of 22 nm. The excitation monochromator has a resolution of 0.2 nm for all measurements.

Figure 4 shows the emission spectra of five $Gd_2O_3:Eu^{3+}$ deposited cluster samples together with a bulk one at a wavelength (190 nm) ensuring an excitation of the host matrix. We observed two different families of spectra. For the unannealed sample and the sample annealed below 425 °C the spectra (not shown for clarity) resemble those reported in the literature as "cubic disordered" samples.[14] On the other hand for higher annealing temperatures, the spectra correspond to the bulk cubic phase $Gd_2O_3:Eu^{3+}$. However, one can note a small broadening of the different emission peaks clearly inversely correlated to the size.

Since we wanted to observe the evolution of the gap for the cubic phase gadolinium oxide we considered in the following only those samples which exhibit the emission typical from the bulk, i.e., the one annealed at temperatures above 475 °C. It is worth noticing that for those samples no specific emission from the Eu^{3+} ions at the surface is

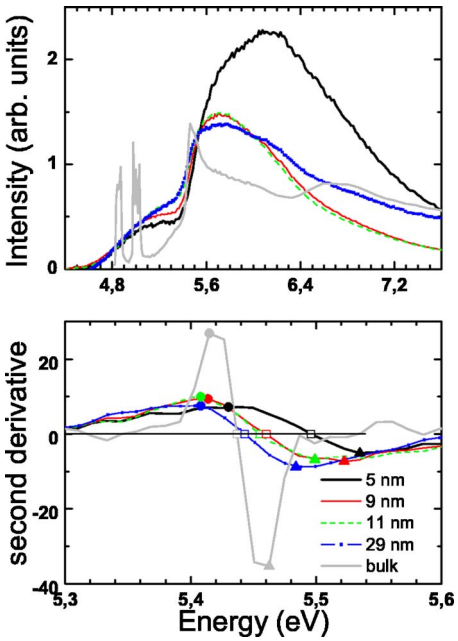

FIG. 5. Upper panel: excitation spectra of nanocrystals annealed at different temperatures monitored at 611 nm and of the bulk sample monitored at 311 nm. Lower panel: second derivative of the excitation spectra in the region of the band gap. The squares denote the inflection point of the excitation spectra while the bullets and the triangles stand for the beginning and the end of the slope, respectively.

observed contrary to what we have observed for other synthesis methods.[8] Therefore we are sure that we observe only the emission coming from europium ions inside the nanocrystal. The excitation spectra for both clusters deposited and bulk samples are presented in Fig. 5.

The excitation spectrum of the bulk sample when going from low to high energies shows a series of lines corresponding to different $f-f$ transitions of Gd^{3+} $^8S_{7/2} \rightarrow {}^6I_J$ (around 4.5 eV) and $^8S_{7/2} \rightarrow {}^6D_J$ (between 4.8 and 5.15 eV) and clearly exhibits a sharp increase in the signal around 5.4 eV which is assigned to the transition between valence and conduction bands and therefore gives the gap of the bulk system. For the annealed cluster deposited samples, the spectra exhibit a large band around 5.1 eV associated with the charge transfer band of europium and then an increase in the spectra around 5.4 eV once again associated with the valence to conduction band transition. In the case of the cluster deposited samples we, of course, do not see the transitions of the Gd^{3+} ion since they are orders of magnitude lower in absorption cross section than both the charge transfer and the band to band transition. This is all the more significant as we are dealing with thin film deposits.

The changes in gap position are expected to be in the order of 0.1 eV for the sizes we are considering. The lower panel of Fig. 5 presents the second derivative of the excitation spectra zoomed in the region of the band to band transition. We assigned the gap value to the inflection point in the excitation spectra, so, in the second derivative curve, to the point which crosses the abscissa axis. This allows a more precise determination of the gap with a precision better than 0.01 eV (0.1 nm in this wavelength range). This point has been denoted on the figure by empty squares. We have also stressed out the maximum and minimum of the curves which denote the beginning and end of the slopes.

At this point it is necessary to discuss the method of evaluation of the gap of the material through excitation spectra. When performing an excitation spectrum one sees the result of a three step process: the absorption of the incoming photon, the transfer of the excitation to the luminescent center, and the emission of the luminescent center. What we are interested in is the absorption of the matrix. Since the emission spectra, apart from the natural broadening of the lines, do not change with the size of the particles as evidenced by the spectra of Fig. 4 we can assume that no change in the emission of the luminescent center as a function of the size happens. So the main point is to know whether there are any changes in the process of transferring the excitation from the matrix to the luminescent center. This can happen if there are some new radiative or nonradiative centers which appear at low sizes (quenching centers at the surface, defects,…). In this case the overall excitation spectra in the part assigned to the matrix will decrease but the shape will not change and then the way we evaluate the change in the gap will not be affected. The last possibility is that some specific absorption near the gap edge is de-excited preferentially towards another center than our luminescing probe (for instance, some excitonic absorption which could transfer preferentially to the europium when the size increases or decreases). If this was the case we would observe a peak in the excitation spectra which would deepen or increase when the size decreases. It is clearly not the case in the spectra of Fig. 5. It is also worth noting that this method has already been used for semiconductor particles (ZnS) for which quantum confinement was also observed through other means.[19] So by using this method we can evaluate changes ΔE_g in the gap even though we do not extract exact values of the gap. In a previous paper[8] we reported evolutions of the gap for Gd_2O_3 through excitation spectra which were higher. At that time the spectra were not clean enough to extract an inflection point in the curve and we could only compare the maxima of the excitation spectra, which would be comparable here with the end of the slope. In other words at that time we were giving more weight to the smallest sizes in the size distribution for a given sample. Indeed the changes observed at that time are of the same order of what is observed for the changes in the end of the slope (up triangle on Fig. 5). The use of the inflection point gives a more accurate value since it averages over the whole size distribution.

The values of ΔE_g derived by this method are reported in Fig. 6 and compared to the evolution observed for other materials, silicon, CdS, ZnO, and CuBr both experimentally and theoretically. For all materials the evolution follows a power law with an exponent equal to approximately 1.4 even though the ionicity, band gap, or static dielectric constant are very different as can be seen on Table II.

V. DISCUSSION

Highly ionic materials are somehow intermediate between purely covalent materials such as Si and van der Waals

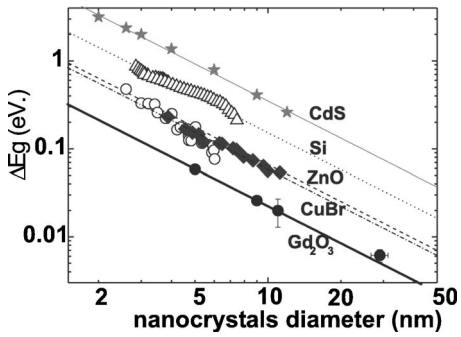

FIG. 6. Variation of the gap of nanocrystals of different materials both experimentally [CdS ∗ (Ref. 20), Si (Ref. 23) Δ, ZnO (Ref. 24) ○, CuBr (Ref. 21) ♦, and Gd_2O_3 (this work) •] and theoretically [Si (Ref. 5) (dotted line) and ZnO (Ref. 24) (dashed line)]. The other lines are guides for the eyes.

materials such as rare gas solids. In the van der Waals solid one can pretty well describe the condensed phase as a collection of gas-phase species. In covalent materials, on the opposite, the strong interaction between atoms imposes to explain the properties of the solid in terms of many body interactions. This leads therefore to the very sensitive nature of covalent materials towards size effects.

For ionic materials as stated by Madden and Wilson,[25] "The ions themselves are profoundly influenced by their environment… the interaction of one ion with another cannot be expressed without reference to the environment in which each ion is found." So we would also expect some size effects to appear.

Although the evolution of the gap with size we observe seems to follow a similar behavior as for other more covalent materials, one cannot discard immediately other effects. In particular, since we are dealing with very small particles, they are very sensitive to stress which might modify the lattice parameter and henceforth the gap of the material. This effect can be estimated here. On Fig. 3 we observe a very small variation of the position of the diffraction peaks. For instance, for the (222) line we see a shift of 1/10 of a degree. This would imply a shift in the lattice parameter of 0.1%. Xu *et al.*[26] have calculated the variation of the gap of Y_2O_3 with the volume of a unit cell. Although it is not the same material, we believe the variation should be of the same order of magnitude since they are very close. By using their calculation, the gap variation induced by the change in lattice parameter for the smallest particles we are considering should be in the order of 6 meV. As shown on Fig. 6 the variation we measure is 50 meV, almost one order of magnitude higher. So it seems reasonable to search the origin of this variation somewhere else.

Konrad *et al.*[27] have observed the evolution of the diffuse reflection spectra of Y_2O_3 samples made by chemical vapor deposition. From the analysis of their data they deduced important shifts of the gap for small particles. However, their determination of the gap is not easy since they deduce it from reflection spectra which include both the variation of the index of refraction and the extinction coefficient. Since the index of refraction also changes strongly near the extinction edge, the position of the gap is generally blurred by this method. They also used excitation spectra of the intrinsic Y_2O_3 exciton and then fitted the edge by a Gaussian. This gives generally the position of the exciton absorption in a bulk material. But since they are dealing with an ensemble of small particles with unknown size distribution this method will favor the smallest particles of the whole.

For many of the materials that we used in the comparison of Fig. 6, theoretical calculations have been made. In the EMA for a two dimensional system or for a three dimensional system with spherical symmetry, the changes of the valence to conduction band as a function of size can be described by the following rule:

$$\Delta E_{\mathrm{exc}} = \frac{2\hbar^2\pi^2}{d^2}\frac{1}{m^*_{e-h}} - \frac{3.572e^2}{\epsilon_0 d}, \tag{1}$$

d being the diameter of the particle, m^*_{e-h} the reduced mass of the exciton, and ϵ_0 the static dielectric constant of the material.

In (1) the first term corresponds to the energy of a particle in a potential well and the second to the Coulomb interaction.

In the real case of a three dimensional material without spherical symmetry there is no analytical solution to the problem. In order to estimate the variation of the gap with the size one has to calculate for different sizes the band structure of the nanoparticles and then fit the data with an empirical law. This has been done, for example, in the case of silicon, zinc oxide, CdSe, or CuBr and the resulting curves are presented in Fig. 6. The theoretical values fairly reproduce the experiments as can be seen from the comparison of the theoretical curve and the experimental data collected from different authors.

Interestingly, for all these materials, the variation is observed to follow roughly the same kind of law, $\Delta E_{\mathrm{gap}} = \alpha/d^{\gamma}$ with the same γ exponent, $\gamma \sim 1.4$. From Eq. (1) we also expect that α should depend on the effective mass and on $1/\epsilon_0$.

For Si, ZnO, CdS, and CuBr, values of the effective mass and ϵ_0 can be found in the literature.[5,7,20,21] They are reported on Table II. From the slope of the curves of Fig. 6, we can also have the value of α for all these materials (also reported on Table II). If we now plot α as a function of the effective mass as presented in Fig. 7 we observe a linear evolution

TABLE II. α coefficient from Eq. (2), static dielectric constant (ε_0), bulk gap value (E_g), and Bohr radius (R_B) in Si, ZnO, CdS, CuBr, and Gd_2O_3.

Material	α	ε_0	E_g (eV)	m^*_{e-h}/m_e	Ionicity
Si	3.73[a]	11.6[a]	1.17[a]	0.138[a]	0
ZnO	1.67[b]	8[b]	3.7[b]	0.227[b]	0.616[c]
CdS	8.78	5[d]	2.5[d]	0.085[d]	0.685[c]
CuBr	1.47	7.9[e]	3.07[e]	0.201[e]	0.735[c]
Gd_2O_3	0.56	16[f]	5.44	0.25	0.9

[a]Reference 5.
[b]Reference 7.
[c]Reference 9.
[d]Reference 20.
[e]Reference 21.
[f]Reference 22.

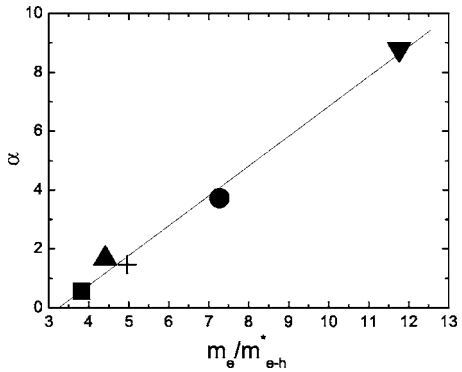

FIG. 7. Variation of α as a function of the ratio m_e/m^*_{e-h} for four materials (• Si, ▼ CdS, + ZnO, and ▲ CuBr) as well as the value deduced from the model (line) for ■ Gd_2O_3

$$\alpha = 1.02 \times \frac{m_e}{m^*_{e-h}} - 3.4 \quad (2)$$

between the four materials from the literature. In this last equation m_e is the mass of an electron. In the case of Gd_2O_3 the evolution of the gap also shows a very similar behavior as can be evidenced by the experimental values reported in Fig. 6, with exactly the same slope, γ. We can then extract a value of $\alpha=0.56$ and by using Eq. (2) leads us to a value of the effective mass $m^*_{e-h}=0.25\times m_e$.

If we come back to the lower panel of Fig. 5, we also pointed out the points corresponding to the beginning of the slope and the end of the slope (bullets and up triangles). It is interesting to note that they also move with the size of the particles. In particular, the beginning of the slope moves very slowly while the end on the contrary changes strongly. Just after synthesis and before annealing the particles have a typical size dispersion of 3.5 nm±15%. After annealing the dispersion is probably enhanced. This is evidenced by the two HRTEM images on Fig. 2. For this particles of 4.5 nm mean diameter we find particles of 3.5 up to 10 nm. Therefore since we have some dispersion it is logical that the slope is broadened and we can evaluate the amount of broadening expected. For instance for the particles of 5 nm mean diameter considering the shift of both minima and maxima of the second derivative, the size dispersion should be between 4 and 12 nm. This is quite reasonable compared to the results by HRTEM. For 29 nm particles it leads to size between 11 and 50 nm which is also quite reasonable.

Gadolinium oxide is a rather ionic material. From Phillips[9] we can evaluate its ionicity to be ~0.9. For such ionic materials the exciton is no more a Mott-Wannier exciton but a Frenkel exciton.[4,28] For this second type of exciton, we would not expect the same kind of variation with sizes as for semiconductors but something like the behavior observed in rare gas clusters.[6] Nevertheless the confinement effect we observe is closer to the one on semiconductors as evidenced by Fig. 6. In the effective mass approximation model, the curvature of both conduction and valence bands are connected to the amplitude of the gap shift, and even in highly ionic materials so orbital overlap is present which gives rise to some curvature of the bands. It means that even without a Mott-Wannier exciton, the confinement should appear on the valence and conduction bands. Then assuming that we observe this gap shift we can define a radius for which this confinement starts to be operative. In the frame of the EMA approximation this radius is given by $R=a_0(\epsilon_0 m/m^*_{e-h})$ where a_0 is the Bohr radius for hydrogen $a_0=\hbar^2/2me^2=0.051$ nm. For Gd_2O_3 according to our results this radius would be 3.12 nm. We believe that what we observe here is only the consequence of the confinement over the covalent part of the atomic bonds. The band diagram of a material and, in particular, the energy extension of the conduction or valence band is directly related to the degree of ionicity of the material. In very ionic materials such as NaCl the valence band is only a few tens of eV wide. Therefore the confinement can only induce small changes in the gap. Nevertheless these changes will be induced by the small covalency of the material. The radius that we have defined is probably indicative of a distance for which the confinement effects on the covalent part of the bonding becomes significant.

In a complimentary way it would be interesting in the future to look at the evolution of the position of the Frenkel exciton absorption in the same kind of material by looking at the emission of the self-trapped exciton and see if its variation is closer to that of Frenkel excitons in rare-gas clusters.

If our simple model is true, however, it gives a general way to estimate quantum confinement effects on the gap of materials.

VI. CONCLUSION

From the evolution of excitation spectra of a dopant (Eu^{3+}) inside Gd_2O_3, the shift of the band gap of this material as a function of the size has been estimated. It follows a trend which is also observed for materials as different as Si, CdS, ZnO, or CuBr. A general empiric rule could be derived from these results giving a way to compare the effect of confinement in materials. Our results go to show that quantum confinement is operative also for ionic materials. This is to be further confirmed on other highly ionic materials.

This work was supported by the European Community-Research Infrastructure Action under the FP6 "Structuring the European Research Area" Programme through the Integrated Infrastructure Initiative "Integrating Activity on Synchrotron and Free Electron Laser Science." This work has been partly carried out at the CIRA (Centre Interlaboratoire de recherché sur les agregats) and partly supported by the BQR from the Université Claude Bernard Lyon 1. The authors are very thankful to Gregory Striganyuk for his invaluable help on the Superlumi line of DESY

[1] A. L. Efros and A. L. Efros, Sov. Phys. Semicond. **16**, 772 (1982).
[2] L. E. Brus, J. Chem. Phys. **80**, 4403 (1984).
[3] M. Bruchez, M. Moronne, P. Gin, S. Weiss, and A. P. Alivisatos, Science **281**, 2013 (1998).
[4] C. Kittel, *Introduction to Solid State Physics* (Wiley, New York, 1986).
[5] C. Delerue, G. Allan, and M. Lannoo, Phys. Rev. B **48**, 11024 (1993).
[6] T. Laarmann, K. von Haeften, A. Kanaev, H. Wabnitz, and T. Möller, Phys. Rev. B **66**, 205407 (2002).
[7] T. Makino, N. T. Tuan, H. D. Sun *et al.*, Appl. Phys. Lett. **78**, 1979 (2001).
[8] B. Mercier, C. Dujardin, G. Ledoux, C. Louis, O. Tillement, and P. Perriat, J. Appl. Phys. **96**, 650 (2004).

[9] J. C. Phillips, Rev. Mod. Phys. **42**, 317 (1970).
[10] B. Bihari, H. Eilers, and B. M. Tissue, J. Lumin. **75**, 1 (1997).
[11] S. P. Feofilov, A. A. Kaplyanskii, R. I. Zakharchenya, Y. Sun, K. W. Jang, and R. S. Meltzer, Phys. Rev. B **54**, R3690 (1996).
[12] A. Huignard, V. Buissette, A. C. Franville, T. Gacoin, and J.-P. Boilot, Chem. Mater. **14**, 2264 (2002).
[13] V. Buissette, A. Huignard, T. Gacoin, J.-P. Boilot, P. Aschehoug, and B. Viana, Surf. Sci. **532–535**, 444 (2003).
[14] B. M. Tissue, Chem. Mater. **10**, 2837 (1998).
[15] R. S. Meltzer, K. W. Jang, K. S. Hong, Y. Sun, and S. P. Feofilov, J. Alloys Compd. **250**, 279 (1997).
[16] B. Masenelli, P. Melinon, D. Nicolas *et al.*, Eur. Phys. J. D **34**, 139 (2005).
[17] M. Pellarin, C. Ray, J. Lermé, J. L. Vialle, M. Broyer, and P. Mélinon, J. Chem. Phys. **112**, 8436 (2000).
[18] K. Wandelt and C. R. Brundle, Surf. Sci. **157**, 162 (1985).
[19] L. Chen, J. H. Zhang, S. Z. Lu, X. G. Ren, and X. J. Wang, Chem. Phys. Lett. **409**, 144 (2005).
[20] M. V. R. Krishna and R. A. Friesner, J. Chem. Phys. **95**, 8309 (1991).
[21] K. K. Nanda, F. E. Kruis, H. Fissan, and S. N. Behera, J. Appl. Phys. **95**, 5035 (2004).
[22] D. Landheer, J. A. Gupta, G. I. Sproule, J. P. McCaffrey, M. J. Graham, K.-C. Yang, Z.-H. Lu, and W. N. Lennard, J. Electrochem. Soc. **148**, G29 (2001).
[23] G. Ledoux, J. Gong, F. Huisken, O. Guillois, and C. Reynaud, Appl. Phys. Lett. **80**, 4834 (2002).
[24] R. Viswanatha, S. Sapra, B. Satpati, P. V. Satyam, B. N. Dev, and D. D. Sarma, J. Mater. Chem. **14**, 661 (2004).
[25] P. A. Madden and M. Wilson, Chem. Soc. Rev. **25**, 339 (1996).
[26] Y.-N. Xu, Z. Q. Gu, and W. Y. Ching, Phys. Rev. B **56**, 14993 (1997).
[27] A. Konrad, U. Herr, R. Tidecks, F. Kummer, and K. Samwer, J. Appl. Phys. **90**, 3516 (2001).
[28] M. Fox, *Optical Properties of Solids* (Oxford University Press, New York, 2001).